On the fluidization of cohesive powders

Differences and similarities between micro- and nano-sized particle gas–solid fluidization

Kamphorst, Rens; Wu, Kaiqiao; Salameh, Samir; Meesters, Gabrie M.H.; van Ommen, J. Ruud

DOI
10.1002/cjce.24615

Publication date
2022

Document Version
Final published version

Published in
Canadian Journal of Chemical Engineering

Received: 16 January 2022 | Revised: 10 April 2022 | Accepted: 12 April 2022

DOI: 10.1002/cjce.24615

SPECIAL ISSUE ARTICLE

THE CANADIAN JOURNAL OF CHEMICAL ENGINEERING

On the fluidization of cohesive powders: Differences and similarities between micro- and nano-sized particle gas–solid fluidization

Rens Kamphorst[1] | **Kaiqiao Wu**[1] | **Samir Salameh**[2] | **Gabrie M. H. Meesters**[1] | **J. Ruud van Ommen**[1]

[1]Department of Chemical Engineering, Technical University Delft, Delft, The Netherlands

[2]Department of Chemical Engineering, Fachhochschule Münster, Münster, Germany

Correspondence
Rens Kamphorst, Department of Chemical Engineering, Technical University Delft, van der Maasweg 9, Delft, 2629HZ, The Netherlands.
Email: r.kamphorst@tudelft.nl

Funding information
ARC-CBBC; Netherlands Ministry of Economic Affairs; Dutch Research Council (NWO)

Abstract

The fluidization of cohesive powders has been extensively researched over the years. When looking at literature on the fluidization of cohesive particles, one will often find papers concerned with only micro- or only nano-sized powders. It is, however, unclear whether they should be treated differently at all. In this paper, we look at differences and similarities between cohesive powders across the size range of several nanometres to 10s of micrometres. Classification of fluidization behaviour based on particle size was found to be troublesome since cohesive powders form agglomerates and using the properties of these agglomerates introduces new problems. When looking at inter-particle forces, it is found that van der Waals forces dominate across the entire size range that is considered. Furthermore, when looking into agglomeration and modelling thereof, it was found that there is a fundamental difference between the size ranges in the way they agglomerate. Where the transition between the types of agglomeration is located is, however, unknown. Finally, how models are made and agglomerate sizes are measured is currently insufficient to accurately predict or measure their sizes consistently.

KEYWORDS

aggregation, cohesion, fluidized bed, inter-particle forces, nanopowder

1 | INTRODUCTION

The applications of micro- and nano-sized particles are widespread: food,[1–4] biomedical applications,[5,6] water treatment,[7,8] sensors,[9,10] and electronic devices[11,12] to name only a few. With even more possible applications being researched, the processing of these powders is a field worth looking into. Gas–solid fluidization is often the preferred option for processing powders.[13,14] In this system, a gas flows through a bed of powder, creating drag, which lifts the particles, resulting in a liquid-like phase.[15,16] This process is relatively straightforward when considering particles in a range of roughly 30 μm to 1 mm, but becomes tougher when using smaller particles due to cohesive inter-particle forces starting to dominate. A lot of studies have been published on the fluidization of cohesive powders, but most of them are focused on either micro- or nano-sized particles. It is

unclear, however, whether a sharp distinction should be made between the two and, if so, what the differences in their fluidization behaviour are and what causes these differences.

In this study, a review of literature on the characteristics of cohesive powders in a fluidized bed is given, with a focus on studies published in the last 20 years. We touch upon the classification of fluidization behaviour based on particle properties and inter-particle forces. We look at which forces dominate for micro- and nano-sized particles as well as which equations are typically used to describe the forces on both scales. Additionally, formed agglomerates from powders in the two size ranges are compared and models to predict their sizes are discussed.

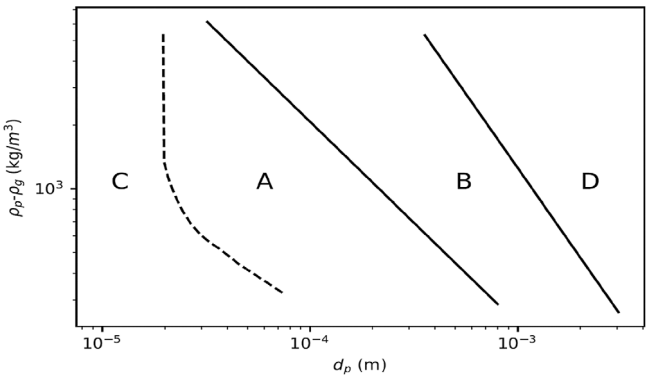

FIGURE 1 Geldart diagram (recreated from the work of Geldart[30])

2 | POWDER CLASSIFICATION

Over the years, many ways of classifying powders, with respect to their fluidization behaviour, have been developed. For the completeness of this work, a brief overview is given of the classifications of non-cohesive powders.

2.1 | Particle size

Before any classification with respect to fluidization behaviour can be done, we need to establish when a powder is called 'micro' or 'nano'. Wang et al. defined nanoparticles as 'powdered materials with individual particles in nanometre scale'.[17] This definition becomes problematic, however, when considering a three-dimensional particle with a high aspect ratio, resulting in the particle having dimensions at both micro- and nanoscale. Examples of this include carbon nanotubes[18,19] and asbestos.[20,21]

In their 2011 report, the European Commission stated: 'Nanomaterial means a natural, incidental or manufactured material containing particles, in an unbound state or as an aggregate or as an agglomerate and where, for 50% or more of the particles in the number size distribution, one or more external dimensions is in the size range 1–100 nm'.[22] This definition addresses both the aspect ratio of individual particles as well as particle size distribution. It is known that powder consisting of particles of different size ranges exhibits distinct, usually improved, fluidization behaviour, not only for cohesive powders that consist of both nano- and, cohesive, micro-sized particle,[23,24] but also of non-cohesive powders mixed with fine powder.[25–29] For this paper we will use the following definition for nanopowder: A powder that consists of primary particles of which at least one external dimension is smaller than 100 nm, where it is assumed that the average particle size can be used to describe all the particles the powder consists of.

A definition like this for micropowders is not as simple, since it is not their size but their behaviour upon fluidization, which is of interest. We are only considering cohesive particles, to avoid tediously restating this over and over, the term 'microparticles' will, in this work, exclusively refer to particles in the micro-size range that fall in the Geldart type C classification (see Section 2.2), typically being smaller than 30 μm. When trying to fluidize these powders, they agglomerate and form channels, often requiring additional equipment to initiate fluidization.

2.2 | Geldart diagram

The most well-known classification for the fluidization of powders, based on size and density, was proposed by Geldart in 1973.[30] He performed fluidization experiments with sieve fractions of several powders and looked at minimum fluidization velocity, minimum bubble velocity, bed voidage, and bed height expansion to find the influence of particle properties on fluidization behaviour. The resulting classification is shown in Figure 1. Powders are classified as type A when they fluidize easily, give large bed expansions and start bubbling at a superficial gas velocity far above the minimum fluidization velocity. Type B powders are also easy to fluidize but start bubbling at, or close to, the minimum fluidization velocity. Type C powders tend to stick together and form plugs, agglomerates (sometimes called clusters), and channels. In general, these powders cannot be fluidized without the aid of assistance methods. Type D powders are spoutable materials: upon

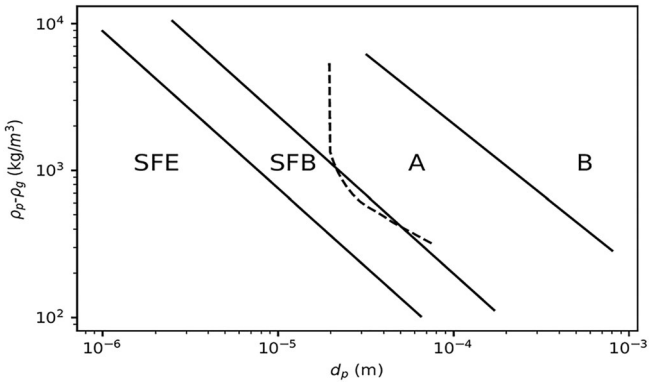

FIGURE 2 Extended Geldart diagram (recreated from the work of Valverde and Castellanos[34]). SFB, solid-like to fluid-like to bubbling. SFE, solid-like to fluid-like to elutriation

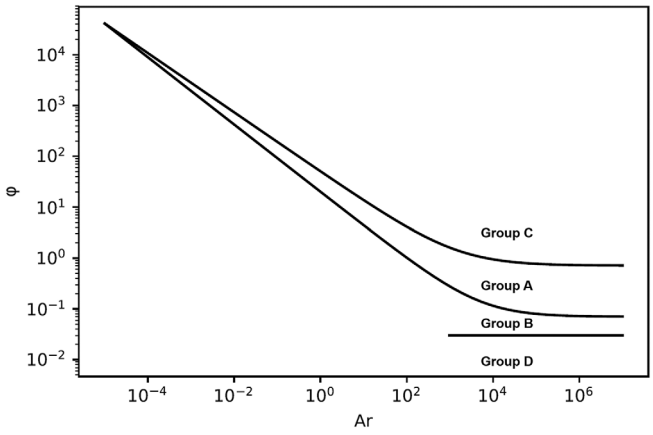

FIGURE 3 Geldart classification based on Archimedes number (Ar) and dimensionless inter-particle forces (recreated from the work of Mostoufi[39])

the introduction of a gas flow a spouted bed can be formed. This is not considered fluidization, since the particles do not form a consistent phase with bed expansion and/or bubbling. Whereas the boundaries between type A and B and type B and D were calculated, the shaded line, separating type A and type C powders, is drawn based on empirical data.[30] The Geldart diagram is still widely used, since it gives a reasonable prediction of fluidization behaviour based on few, and easily accessible, properties.

Particles of interest for this paper are all type C and should therefore, according to the diagram, have the same fluidization behaviour. However, the smallest sieve fraction used by Geldart was 10–20 μm,[30] meaning smaller particles could show different behaviour upon fluidization. This would then require an extension of the diagram to make an accurate prediction of the fluidization behaviour of powders within the type C size range possible.

2.3 | Extension of the Geldart classification

Although Geldart's diagram is a useful tool, it is not always applicable to fine (micro-sized) and ultra-fine (nano-sized) powders, some of which can be fluidized without using assistance methods, despite the diagram predicting the opposite.[31–33] Valverde and Castellanos developed an extension of the Geldart diagram, as shown in Figure 2. Solid-like to fluid-like to bubbling (SFB) and solid-like to fluid-like to elutriation (SFE) are identified as distinct fluidization regimes.[34] It is important to note here that the d_p on the x-axis of Figure 2 is not the diameter of the primary particle but of pre-existing simple agglomerates. The graph therefore uses the well-known phenomena in fluidization of fine powders, that not the primary particles but the formed agglomerates dominate the fluidization behaviour.[31,35]

2.4 | Classification based on inter-particle forces

The diagram proposed by Geldart shows the type of fluidization that is expected to happen when air at atmospheric pressure and ambient temperature is used as the fluidizing gas. Grace was among the first to propose using a generalization based on the Archimedes number[36] (Ar) (the ratio between gravitational and viscous forces) in order to include different gases and pressures, which was later adopted by several other studies.[37,38] Using Ar, the viscosity of the fluidization medium is included.

$$\mathrm{Ar} = \frac{g d^3 \rho_f \left(\rho_p - \rho_f\right)}{\mu^2} \tag{1}$$

For the calculation of Ar for cohesive powders using d and ρ_p as constants of the primary particle or of the formed agglomerates will change the result. Most studies do not explicitly mention which one to take,[37–39] some use the primary particle properties.[36,40] Since the fluidization behaviour of fine powders is known to be dominated by the formed agglomerates[31,35] one could argue that, for fine powders, the properties of agglomerates should be taken instead.

Recently, Mostoufi proposed a generalization that includes predictions of the type of fluidization that should be expected when assistance methods are used. This diagram is based on the dimensionless inter-particle force (φ) and Ar,[39] see Figure 3.

where φ is defined as:

$$\varphi = \frac{F_{IP}}{F_W - F_B} \quad (2)$$

where F_{IP} is the sum of all attractive inter-particle forces minus the repulsive inter-particle forces which include forces that are introduced by assistance methods. This is, however, not straightforward, since there is a discussion on which forces are relevant on which scale and on how they should be calculated, as will be discussed in Section 3. F_W and F_B are the forces resulting from the weight of the particle and the buoyancy, respectively. From this, it can be seen that using assistance methods to fluidize cohesive powders will decrease the value of φ by introducing a repulsive force that reduces the value of F_{IP} and therefore causes a transition from type C to type A fluidization when enough repulsive force is introduced. It is important to note that in Figure 3, the correlation between primary particle size and fluidization type is indirectly found in the Ar since agglomerate size depends on primary particle size, as will be discussed in Section 4. The dimensionless interparticle force (Equation (2)) is also a function of primary particle size, as will be discussed in Section 3.

2.5 | Limitations of the classification of cohesive powders

Since cohesive powders form agglomerates, it is often unclear whether the agglomerate size or the primary particle size should be used for predicting the fluidization behaviour. Considering that the agglomerates dominate the fluidization behaviour,[31,35] taking the agglomerate properties seems to be the best option. This does, however, introduce other complications. First of all, agglomerates have large size distributions.[41–45] This might seem trivial to point out since one can just use the average agglomerate size when classifying the powder; however, it is also known that mixtures of powders with different sizes significantly change the fluidization behaviour.[46–48] Second, using agglomerate size to predict fluidization behaviour is complicated further since agglomerates are not evenly spread through the bed but larger ones are more often found at the bottom whereas smaller ones are found at the top.[49,50] Third, agglomerate size was found to depend on fluidization time[51] (see Section 4.2). Another complication appears when looking at Equations (1) and (2). It is important to be aware that assistance methods are commonly thought to break up agglomerates (see Section 4.4), and therefore decreasing the value of Ar. Assistance methods are also introducing repulsive forces which will decrease the value of φ. Looking at Figure 3, this makes assistance methods effective in two ways when it comes to making type C powders behave like type A ones. This can mean one of two things: Either the introduction of assistance methods has a high effectiveness for the improvement of fluidization by decreasing both Ar and φ aspects, or the effect of the assistance method is overestimated since it is introduced twice using this method. This can either mean that the primary particle size should be used to calculate Ar, which contradicts the idea that agglomerates dominate fluidization behaviour, or that this method is not valid for accurately predicting assisted fluidization behaviour of particles that form agglomerates.

3 | FORCES ACTING ON PARTICLES

The different forces acting on particles in a fluidized bed are the causes of the fluidization behaviour and resulting agglomeration.[33,52] Therefore, we will highlight these forces in this chapter. Forces acting between particles directly, Figure 4, ones acting between particles and fluidization gas, and collisions are considered.

Agglomeration is the result of the interplay of cohesive and repulsive forces.[41] The forces that are typically considered to act between particles that form the agglomerates are[53,54]: gravity, drag force, van der Waals forces, capillary force, electrostatic force, and forces due to collisions. They will all be introduced shortly in this review; for more extensive descriptions of the forces that dominate fluidization, see the works of van Ommen et al., Tahmasebpoor et al., Seville and Willett, Leroch and Wendland, and Endres et al.[13,54–58]

3.1 | Gravitational force

The most obvious force that must be overcome to fluidize a powder is gravity or weight force. Since gravity acts on the volume of a body, it can mostly be neglected for fine powders whereas inter-particle attraction which works on the particle surfaces becomes much more important. Basically, at a scale of hundreds of micrometres, this surface/volume effect becomes relevant, meaning that the formed agglomerates have enough mass to experience gravity as a significant force counteracting the gas flow. For a spherical particle, the gravitational force can be calculated by:

$$F_W = \frac{\pi}{6}\rho_p g d_p^3 \quad (3)$$

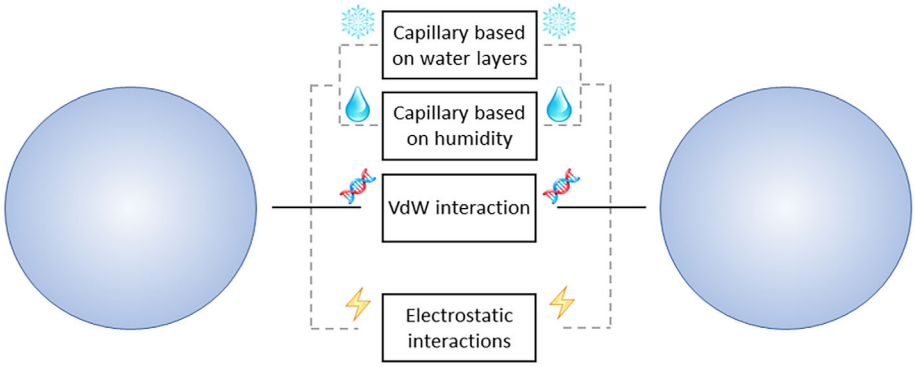

FIGURE 4 Forces acting between particles. vdW, van der Waals

Note that in Equation (3), ρ_p and d_p are the density and diameter of the primary particle, respectively. When calculating F_W for agglomerates, the density and diameter of the agglomerate should be taken instead.

Buoyancy is sometimes used in relation to agglomerate size, but due to the low density of the fluidizing gas compared to that of the particles, the effect of buoyancy is low. When considering agglomerates, one could argue that buoyancy should be taken into account, since the agglomerates have an open structure and therefore a low density. However, buoyancy usually is neglected when it comes to particles/agglomerates in a gas.

A relation that is commonly used in literature related to the weight force to the inter-particle force is the Bond number.

$$\mathrm{Bo} = \frac{\Sigma F_{\mathrm{cohesive}}}{F_W} \tag{4}$$

When $\mathrm{Bo} > 1$, the powder is considered cohesive.[59] Note here that, since F_W scales with d_p to the power three and cohesive forces typically scale with a lower power, the Bond number decreases with increasing particle size, meaning the particles become less cohesive, which is in agreement with the classifications discussed earlier.

3.2 | Drag force

The drag force creates lift which, when exceeding the gravitational pull, makes particles or agglomerates fluidize. While particles or agglomerates are fluidized, the drag force is usually assumed to be equal to the buoyant weight.[60,61]

The general expression for drag force, using Stokes law in the laminar regime, is given by:

$$F_D = 3\pi\mu d_p u \tag{5}$$

For particles lifted by a gas flow in the laminar regime in a suspension of alike particles, the equation can be generalized[62]:

$$F_D = 3u\pi\mu\varepsilon^{-3.8} d_p \tag{6}$$

where ε is the void fraction of the bed, which is assumed to be independent of u.[62] This equation is semi-empirical and was confirmed by experiments. The inclusion of ε is needed to correct for the change in interstitial gas velocity due to the presence of particles.

Apart from creating the needed lift for the particles to fluidize, drag can also break larger agglomerates into smaller ones.[63]

3.3 | Van der Waals force

The van der Waals forces are caused by electric dipoles in atoms/molecules, which result in an adhesive force.[54,64] To describe this attraction for particles, Hamaker developed a simple model for two spheres of equal radius, which is frequently used today:

$$F_{\mathrm{vdW}} = \frac{A_H \cdot d_p}{24 H_0^2} \tag{7}$$

where A_H is the Hamaker constant, d_p is the primary particle size, and H_0 is the minimum inter-particle distance. This distance varies from different sources and assumptions while values between ~0.17[65] to ~0.4 nm[66] and even larger can be found in the literature.

It is important to note that the Hamaker constant, and therefore the resulting van der Waals force, is a function of particle size, particle geometry, material, and temperature.[67] This means that for processes at elevated temperatures, like particle coating,[68] the fluidization behaviour might be affected. This effect has been shown

in publications, although it cannot account for all of the differences found in fluidization behaviour at high temperatures.[69,70]

When talking about van der Waals forces between formed agglomerates, Equation (7) cannot be applied directly. However, several approaches to calculate F_{vdW} between agglomerates are found in the literature. First of all, when one assumes agglomerates are very dilute and only a few particles are in direct contact, the van der Waals force between them can be calculated as[71]:

$$F_{vdW} = N \cdot \frac{A_H \cdot d_p}{24 H_0^2} \tag{8}$$

where N is the number of shared particles. The fact that Equation (8) predicts a stronger van der Waals force for bigger particles is, however, inconsistent with the observation made by Matsuda et al. that agglomerates made up of smaller primary nanoparticles are stronger than ones made up of larger nanoparticles.[41,72] However, it is important to note that the number of particles in contact is not equal for different-sized nanoparticles but depends on multiple factors of agglomerate formation.

The second approach is to assume agglomerates are microsized particles with asperities d_{asp}, giving the relation[61,73]:

$$F_{vdW} = \frac{A_H \cdot d_{asp}}{24 H_0^2} \tag{9}$$

where d_{asp} is usually taken as 0.1–0.2 μm.[60,61] Equation (9) is known to overestimate the attractive force between agglomerates made up of nanoparticles due to the assumption that the asperity has no porosity.[41]

To address the shortcomings of the other equations, de Martín and van Ommen proposed Equation (10) to calculate the van der Waals force between two porous agglomerates made up of nanoparticles,[41] which they use to calculate the size of complex agglomerates (see Section 5).

$$F_{vdW} = \frac{A_H \cdot d_a \left(\rho_a/\rho_p\right)^2}{24 z_{eq}^2} \tag{10}$$

where d^* and ρ^* are the diameter and density of the agglomerates, respectively. z_{eq} represents an equivalent distance defined as:

$$z_{eq} = H_0 + k_1 \cdot \mathrm{rms} \tag{11}$$

where k_1 is a coefficient relating the maximum vertical distance between any point of the asperity and the horizontal plane to rms and rms is the root mean square of the surface roughness.[74]

In conclusion, for calculation of the van der Waals force between agglomerates, Equation (9) is thought to be suitable for agglomerates made up of micro-sized primary particles and Equation (10) is likely most suited for agglomerates made up of nanoparticles. It is important to note that these equations consider the fact that agglomerates are built up out of smaller particles but do not take the structure of formed agglomerates into account. Rather, they describe that fact by general property values such as density or porosity.

The influence of van der Waals forces depends strongly on the surface properties of the particles. Powders with polar (hydrophilic) surfaces strongly bind water to their surface, resulting in a strong attractive van der Waals force which is determined by their surface hydroxyl groups.[54,56,75] For the most commonly used nanopowders in research (TiO_2, SiO_2, and Al_2O_3) a significant increase in minimum fluidization velocity is found when polar powder is used instead of apolar powder, which can be attributed to the strong van der Waals interactions of the hydroxyl groups and water molecules.[56] In addition, surface roughness of the contact area is considered essential to evaluate van der Waals force between particles.[58,76] For numerical simulations, the Hamaker model is vastly extended to address effects of surface roughness, such as modifications for asperities on a flat rough surface[77] or submerged below the surface,[74] and a generic model incorporating asperities at multiple scales.[78]

For simulating the dynamics of cohesive particles, due to the presence of singularity in the Hamaker model, certain modified forms have been proposed to avoid the numerical divergence. As aforementioned, it generally assumes that adhesion force plateaus at a minimum contact distance in the order of asperity, that is $f_{vdW} = f(H_0)$ for $H \leq H_0$. More rigorously, the Hamaker correlation can be modified assuming the deformation is negligible. For example, Galvin and Benyahia[79] proposed an alternative to the Hamaker model that allows to avoid the numerical singularity:

$$F_{vdW} = \frac{A_H 2 r_i r_j \left(r_i + r_j + s\right)}{3 s^2 \left(r_i + r_j + s\right)^2} \left[\frac{s\left(2r_i + 2r_j + s\right)}{\left(r_i + r_j + s\right)^2 - \left(r_i - r_j\right)^2} - 1 \right]^2 \tag{12}$$

where s is defined as the distance between their surface, r_i and r_j are the radius of paired particle i and j, respectively.

For softer particles bigger than 10 μm, Johnson et al.[80] proposed the Johnson–Kendall–Roberts (JKR)

model that accounts for the influence of van der Waals forces with a surface energy density γ_s. Different from the Hamaker model, in which particle deformation during contact is negligible when sufficiently small particles are concerned, the JKR model is contact-dependent and used for the modelling of adhesive granular flows where agglomeration occurs:

$$F_{\mathrm{JKR}} = 4\sqrt{\pi\gamma_s E^* a^3} \tag{13}$$

$$\delta = \frac{a^2}{R^*} - 4\sqrt{\frac{\pi a \gamma_s}{E^*}} \tag{14}$$

where γ_s is surface energy, E^* and R^* are the equivalent Young's modulus and equivalent radius, respectively, and a is the contact radius. The Hamaker constant is material-specific and can be correlated to the surface energy γ_s through the force required to break an adhesive contact:

$$A_{\mathrm{H}} = 24\pi\gamma_s H_0^2 \tag{15}$$

The JKR model has also shown to be sufficient to predict the dynamics of relatively large primary particles.[81,82] Besides, according to the JKR theory, a 'pull-off' force, F_{p}, can be derived for the adhesion between particles.

van der Waals forces can be also modelled semi-empirically. To reduce the computational cost in numerical simulations, Weber et al. simplified the van der Waals forces with a square-well potential and validated using a hard-sphere discrete framework to capture rapid granular flows.[83] Nevertheless, mappings between the constructed square-well and the particle properties are required to enable more generic applications. Similarly, Liu et al. proposed a square-force model which conserves the characteristic cohesive energy and maximal cohesive force over the Hamaker model, as a simple yet reasonable substitute for more rigorous models.[84]

3.4 | Capillary forces

For polar particles, water molecules will adsorb to the particle surfaces. When these particles get close to each other, the water on their surfaces will form a meniscus between them, which introduces an additional attractive force, the capillary force. Hydrophobic particles will have less water adsorbed on their surface, leading to a smaller capillary force.[85]

The capillary force, for a simple two-sphere case, can be expressed as[86]:

$$F_{\mathrm{cap}} = 2\pi\gamma l - \pi l^2 \Delta P \tag{16}$$

where γ is the surface tension of the liquid, l is the azimuthal radius, and ΔP is the pressure difference between the phases. This pressure difference is often calculated using the Young–Laplace and Kelvin equations.[57,86,87] The Kelvin equation was however found to only be valid for particles larger than 1 μm.[88] For smaller particles, some of the assumptions made are no longer valid and new models are needed to describe the forces. The reason for this is twofold. First of all, for micro-sized particles, it can be assumed that the radius of the water meniscus is constant since the radius of the particle is significantly larger than that of the meniscus.[88] For particles smaller than 1 μm this assumption no longer holds. Also, for nanoparticles, the distance between the particles significantly influences the resulting capillary force,[89] whereas this is not so much the case for microparticles. Second, at the nano-scale, the adsorbed water on the particle surface can no longer be treated as a continuum, but individual water molecules should be considered.[88,90] This also means there is no distinct phase boundary between the water and surrounding gas anymore when one considers this small scale, making accurate modelling of capillary forces on nano-sized particles difficult. Simulations using Large-scale Atomic/Molecular Massively Parallel Simulator (LAMMPS)[91] have shown good results in estimating the capillary force of nanoparticles.[57,90] Alternatively, attempts carried out to indirectly account for the impacts of capillary force by applying a 'wet' restitution coefficient to address the energy dissipation during the contact of wet particles.[92,93] However, such a simple alternative cannot model agglomeration[94] and this 'wet' restitution coefficient varies largely with particle properties and operating conditions.

F_{cap} is, among other variables such as temperature or shape of the particles, a function of relative humidity. Interestingly, the humidity dependency is still today a debate since the literature lists contradictory results which are not fully understood yet.[95–98] Nevertheless, we can say that for micro-sized particle F_{cap} will be the dominant force at higher humidities. Since in most studies dry nitrogen or dry air is used as a fluidizing gas, the powder will be dried and capillary forces can be assumed to be insignificant. However, for nano-sized particles, the adsorbed water layers do not disappear in a dry environment, as long as they are not heated,[85] and the capillary forces still play a significant role. At what scale this effect is no longer relevant is currently unknown.

For dynamic particles linked via liquid bridges, a dynamic dissipative (or viscous) force arises from liquid viscosity, in parallel to capillary forces. It is modelled based on lubrication theory:

$$F_{\mu,n} = \frac{3\pi\mu R^2}{2s} v_n \tag{17}$$

where μ is the liquid viscosity, v_n is the normal component of the relative velocity between particles, R is the particle radius, and s is the separation distance. In a similar fashion to the van der Waals force, the dissipative force reaches a singularity when the two concerned particles are in contact ($s = 0$). Similar to the Hamaker model, a minimum separation distance is assumed on the length scale of surface asperities to prevent any singularity.[99]

3.5 | Electrostatic forces

The electrostatic forces that are typically discussed in literature on the fluidization of fine and ultra-fine powders are the ones generated through triboelectrification. These charges are built up through charge separation, typically associated with the rubbing together of dissimilar or similar surfaces.[100–102] Since the fluidized bed is a highly dynamic system, this charge generation occurs constantly. This results in particles having a similar charge and therefore, in principle, repulsing each other, meaning a higher electrostatic force favours deagglomeration. At the same time, however, charged powder will tend to stick to the column walls, meaning that some of the powder will not be part of the bed anymore. Unlike the other forces acting on particles, the electrostatic force is heavily influenced by the handling of the powder, even before the fluidization starts.[103] Note here that the presence of water or alcohol on a particle surface will mitigate this effect, meaning electrostatic forces are typically only present for hydrophobic particles. This also means that the electrostatic forces can usually be nullified by running the fluidizing gas through a bubbler with water or alcohol before letting it enter the bed. The introduction of a saturated gas into the system does, of course, come at the cost of introducing, or increasing, capillary forces into the system. Also, when applied in a reactor, the introduction of water or alcohol vapour can harm the process by introducing undesired side reactions. Electrostatic forces are typically considered to not be relevant for both nanopowders[13,61,104] or micropowders,[105] although studies have also been shown the inclusion of alcohol vapour in fluidized beds to reduce these forces and improve fluidization.[56,100]

3.6 | Collision force

The final considered force is introduced by collisions between agglomerates. In contrast to the adhesion forces, the collision is mostly empirical and a fundamental physical understanding is missing. To calculate this force, the following expression was proposed by Zhou and Li.[48,106] for the collision force between two agglomerates of equal size:

$$F_C = 0.166\left(\frac{\pi V^6 \rho_a^6}{k^2}\right)^{\frac{1}{5}} \cdot d_a^2 \tag{18}$$

where k is a function of Poisson's ratio and Young's modulus and V is the relative velocity of the agglomerates, which is a function of agglomerate density, bed voidage, and bubble diameter.[106,107] It is assumed here that the agglomerates are elastic bodies.

When simply including this equation as a repulsive force in a balance, one would implicitly assume that all collisions lead to the breakage of the agglomerates. The way for small agglomerates to grow, however, is also due to collisions, meaning not all the forces introduced will lead to breakage. Some particles that collide will just bounce off, some will merge, and others will break.

3.7 | Dominant inter-particle forces

Some publications on inter-particle forces include graphs where the forces are plotted as functions of particle size to show in which size range which forces are dominant.[13,108] While useful for an indication, such graphs could be misleading since particle size is not the only relevant parameter that influences the respective forces. The most significant variable is the humidity in combination with a hydrophilic or hydrophobic surface; if under the given conditions, capillary forces play a role, they are usually dominant and will stay dominant over the entire range of sizes relevant for this study. In absence of capillary forces, van der Waals forces are typically dominant. Electrostatic forces are usually thought to only become significant at larger particle sizes[109,110] than those considered in this study. With increasing particle size, gravity will eventually become the dominant force. In conclusion, for the size range considered in this study, the van der Waals force will be the dominant inter-particle force in the absence of moisture. Especially for hydrophilic particles, where the van der Waals forces are relatively large due to hydrogen bond formation.

When comparing micro- and nano-sized powders, one finds that the same forces are dominant for both powders. The way to calculate the values of these forces does differ, but based on this alone, one cannot conclude that these powders behave differently or the same when fluidized.

4 | AGGLOMERATION IN FLUIDIZED BEDS

Fine and ultra-fine powders fluidize as agglomerates. Larger particles, falling in the Geldart type A, are also known to sometimes form agglomerates, or clusters, upon fluidization.[111–113] The observed fluidization behaviour is dominated by the nature of the agglomerates and not so much by the primary particles directly.[31,35] Therefore, it is interesting to look at the agglomerates formed by powders with primary particle sizes in the nano- and micrometre range and find their similarities and differences, since these could explain differences in fluidization behaviour.

4.1 | Particle structure

For a complete understanding, a distinction needs to be made between agglomeration and aggregation. Though these terms are sometimes used interchangeably in literature, they refer to different phenomena. Agglomeration is the process where bodies cluster together as a result of attractive inter-particle forces, forming agglomerates. Agglomerates are fragile by nature[114] and will constantly break and reform in the fluidized bed.[33,115,116] Aggregation is the process where primary particles form solid bridges, resulting in aggregates. The solid bridges are formed by surface diffusion or sintering.[117–120] This takes place at elevated temperatures and pressure,[121] which are the conditions under which nanoparticles are typically produced. Aggregates cannot be easily split back into their primary particles, making them different than agglomerates. Aggregates have net-like structures, sizes in the hundreds of nanometres, and low densities due to the porous structure.[33] Aggregates are the smallest durable entities existing in the fluidized bed of nanopowders. As a result of inter-particle forces, aggregates can cluster together and form agglomerates during storage and fluidization.

Since micropowders are mostly produced by milling[122,123] and spray drying,[124,125] typically no aggregation takes place. This means that the smallest particles present in the bed are the micro-sized primary particles themselves. Note here that the building blocks of agglomerates formed by micro- and nanopowders are thus significantly different in structure and density; agglomerates from micropowders being formed by primary micro-sized particles and those from nanoparticles by the sintered aggregates.

4.2 | Agglomeration in practice

When we look at the modelling done on agglomeration, some knowledge from experimental studies is required. From experiments, it is known that agglomerates are not homogeneously distributed in the fluidized bed.[49] They are segregated based on their size: The larger ones are found at the bottom of the bed, whereas the smaller ones are found at the top.[49] This makes accurately measuring agglomerate sizes tougher since results will be influenced by the height at which measurements are taken. Furthermore, agglomerates are constantly breaking and reforming,[33,115,116] meaning that, if any equilibrium can be reached, this is a dynamic equilibrium and agglomerates do not stop interacting when reaching an equilibrium size.

Another aspect of agglomeration is that there are signs that it is dependent on fluidization time. Mogre et al. found that agglomerate size and bed height, of 21 nm TiO_2, decreased over time.[51] Nam et al. also found a decrease in bed height with time for nanopowder[115] but did not measure agglomerate size. The small number of studies that show this does not, however, mean that this effect is limited to nanoparticles (unlike Ali et al. claim in their study[126]). When considering the observation by Matsuda et al. that agglomerates made up of smaller nanoparticles are stronger than those made up of larger ones,[72] one should expect most, if not all, agglomerates to decrease in size with longer time spent in the fluidized bed. This would mean that reported agglomerate sizes should be considered with care since the measured size is unlikely to be the equilibrium size if the measurements were taken under the assumption that there was no time dependency. This in turn would affect proposed models based on these measurements. It is therefore crucial that the effect of time spent in the fluidized bed on agglomerate size, and other features, are tested and reported upon.

4.3 | Measuring agglomerate size

Several measurement techniques to determine the size of agglomerates in a fluidized bed have been applied in publications. Measuring agglomerate size can be done either in-situ or ex-situ. Due to the fragile nature of agglomerates, ex-situ techniques have the inherent risk of changing the agglomerates before measuring them. Both removing the agglomerates from the bed, as well as the sample preparation thereafter, are likely to influence the acquired results. Therefore, only in-situ techniques will be discussed here.

A way to measure the agglomerate size that is commonly found in literature is by obtaining images of the agglomerates at the surface of the bed. For this, a laser, a source for illumination, a camera, and software to process the images and estimate the size are used.[35,127]

The benefits of this technique are that the agglomerates are not damaged and that the bed is not disturbed. A downside is that only agglomerate sizes at the surface of the bed (the splash zone) can be measured since the lower region of the bed is too dense. As mentioned before, agglomerates tend to segregate based on size, meaning the splash zone is not representative of the whole bed.

A similar technique was proposed by Quevedo and Pfeffer, here a probe was placed inside the bed, allowing to obtain images from below the splash zone.[128] The advantage is that a more representative result can be obtained. The downside, however, is that the bed is disturbed by the presence of the probe, which could influence the results.

Another in-situ measurement technique was developed by de Martín et al. They placed a settling tube in the fluidized bed and measured the terminal velocity of agglomerates falling inside the tube by filming them with a borescope.[129] Apart from the advantage that agglomerate sizes are not only measured in the splash zone, another advantage is that the density of the agglomerates can be calculated from their velocity. The main disadvantage of the technique is that the bed is disturbed by the presence of the tube, which might affect the results.

All three mentioned methods have their pros and cons, and until more is known about how representative the splash zone is for the entire bed, the methods by Quevedo and de Martín should be concluded to be the most accurate. Since models to predict agglomeration are validated by comparing their output with measured agglomerate sizes, it is crucial that the most accurate measurement methods are used to prevent artefacts from influencing the evaluation of model validity. Furthermore, since multiple measurement procedures are used, it is currently not possible to directly compare results, even if all other conditions are equal. It would be interesting to see a study where the methods are compared to see how their results differ.

4.4 | Assistance methods

Fluidization of powders, consisting of cohesive particles, can be drastically improved when using assistance methods. It is hard to definitively say whether a method is effective over a large range of particle sizes since studies rarely show unsuccessful applications of methods. The number of publications spanning a size range can however be an indication of a method being more effective. For instance, of the studies published on the effectiveness of a (micro)jet, one was found for 30 μm powder,[130] whereas multiple were found in the range of 12–25 nm.[128,131–133] For robust proof of limitations in particle sizes for which methods are applicable, more research is required.

The way most studies conclude assistance methods to work is by introducing additional repulsive forces that counteract the van der Waals force, reducing channelling and agglomeration (mechanical vibration,[115] acoustic vibration,[134] magnetic field,[171] stirring,[46] microjet,[128,132] and pulsed flow[135–137]). This additional force can be included in a force balance when modelling agglomerate size.[105] For a comparison of multiple methods and their effectiveness see[138]; note that only one micro-sized powder is used here, meaning it is unknown to what extent results can be generalized.

5 | MODELLING AGGLOMERATION

Throughout the years, many models for the estimation of agglomerate sizes have been proposed. In this paper, we will focus on some recent models.

In a force balance, cohesive and repulsive forces considered are assumed to be in balance, and the found equation is then solved for agglomerate size, d_a.

5.1 | Considerations for modelling

For nanoparticles, it was found that agglomeration takes place in distinctive steps: primary particles to aggregates (sometimes called sub-agglomerates) to primary or simple agglomerates to complex agglomerates, which is a phenomenon that was discovered by Yao et al.[33] Each stage of the multi-stage agglomeration (MSA) has its own density and fractal dimension.[139] The latter is a more recent insight since a fractal dimension of 2.5 was earlier used for all stages of nanoparticle agglomeration.[115,140,141] No MSA has been described for microparticles, making the final agglomerates present in the fluidized bed of microparticles significantly different.

5.2 | Modelling nanoparticle agglomeration

For nanopowders, models were found based on MSA. These models propose ways to calculate the size of the

complex agglomerates. Usually, the ratio between the densities of each of the respective stages is taken[41,115,142]:

$$\frac{\rho_x}{\rho_y} \propto \left(\frac{d_y}{d_x}\right)^{f(D)} \tag{19}$$

where x and y denote the stages, x being the larger one, and the exponent to the ratio of sizes being a function of the fractal dimension of stage x. The nanoparticles first form aggregates with a fractal dimension of ~2,[41] which combine into primary agglomerates with a fractal dimension of 2.5–2.6,[115,140,143] which then merge to form complex agglomerates with a fractal dimension of 2.3.[143] One of the models based on MSA was proposed by Valverde and Castellanos.[144] In their model, they equate the ratio between the diameter of each stage of agglomeration to the Bond number. Solving this for each of the stages results in a relation for the diameter of the complex agglomerates:

$$d_a = d_p^{0.679} \cdot d_{\text{asp}}^{0.321} \cdot \text{Bo}^{0.365} \tag{20}$$

Note here that the primary particle size, d_p, pops up twice, once explicitly and once hidden in the Bond number. Rewriting the equation to make the d_p completely explicit results in:

$$d_a = d_p^{-0.051} \cdot d_{\text{asp}}^{0.321} \cdot \left(\frac{A_{\text{H}}}{4\pi\rho_p g z_0^2}\right)^{0.365} \tag{21}$$

From Equation (21) it can be seen that a slight decrease in agglomerate size is predicted with an increase in primary particle size. The dependency on d_p arises from the van der Waals force and gravity. The power of −0.051 resulting from size ratios and fractal dimensions of the steps in the multi-stage agglomerates.

Another model based on MSA was proposed by de Martín and van Ommen that, for hydrophobic powder, reduces to[41]:

$$d_a = \left(\frac{\widehat{N} A_{\text{H}} d_{\text{sa}}^{D_1+D_0-5}}{\left(H_0 + 0.063 d_p\right)^2 g_{\text{eff}} d_p^{D_0-3} \rho_p}\right)^{\frac{1}{D_1}} \tag{22}$$

This model is derived by equating the global inter-agglomerate forces to the global drag force.[41] Note that, since drag force is equal to weight force,[60,61] this means that the model is essentially solving Bo = 1. When using Equations (3) and (10) in Equation (4), setting Bo = 1, taking $z_{\text{eq}} = H_0 + 0.063 d_p$, and substituting Equations (23) and (24) (assuming k_0 and k_1 to both be constants equal to 1)[41] one finds Equation (22), where $\widehat{N}$ is a fitting parameter.[41]

$$\frac{\rho_{\text{sa}}}{\rho_p} = k_0 \cdot \left(\frac{d_{\text{sa}}}{d_p}\right)^{D_0-3} \tag{23}$$

$$\frac{\rho_a}{\rho_{\text{sa}}} = k_1 \cdot \left(\frac{d_a}{d_{\text{sa}}}\right)^{D_1-3} \tag{24}$$

Note that in the final equation d_a scales with d_p twice; one term is left over from the ratio in density of simple agglomerates and primary particles in Equation (10), and the other one comes from the used equation for z_{eq}. Since $D_0 < 3$, it cannot be easily seen what the effect of d_p will be on the predicted d_a. Doing a sensitivity analysis reveals that the denominator grows with an increasing value for d_p and therefore the d_a is predicted to decrease. This will be discussed further in Section 5.4.

The model by de Martín and van Ommen (Equation (22)) was later modified by Tahmasebpoor et al. to include differences in polarity of materials[54]; this model does, however, require some empirical data. Tahmasebpoor et al. also proposed that electrostatic forces can play a significant role in the equilibrium size of agglomerates, whereas most found models neglect this force. They try to support their claim with data of fluidized beds where alcohol vapour is introduced, which reduces the repulsive electrostatic force. One could however argue that the introduction of attractive capillary forces during such experiments can also explain the data, without the need to include electrostatics.

In the same paper, Tahmasebpoor et al. propose a simplified model, which does not require data from experiments.[54] Assuming hydrophobic particles, no liquid present, and rewriting the equation, one finds the following equation (note that Equation (25) differs from Equation (16) in the work of Tamahsebpoor et al.[54] even using the additional assumptions listed here. This is a result of Tahmasebpoor et al. missing a factor of $\frac{\pi}{6}$ in their calculation of the drag force), which can be directly compared to the other discussed models:

$$d_a = \left(\frac{A_{\text{H}} d_{\text{asp}}}{4\pi z_0^2 \left(\rho_a - \rho_f\right) g}\right)^{\frac{1}{3}} \tag{25}$$

where the assumption is made that $\rho_a = \rho_b$, the bulk density of the powder. This equation is a result of equating drag force and the van der Waals force; this approach is once more the same as saying Bo = 1 (assuming $\rho_f \ll \rho_a$)

and solving for d_a. This is essentially the same as shown in the study by de Martín and van Ommen[41]; the difference in their results stems from the way the van der Waals force is calculated. Tahmasebpoor et al. use Equation (9), taking a constant value for H_0, which results in Equation (25) being independent of primary particle size completely.

5.3 | Modelling microparticle agglomeration

For the prediction of the agglomerate size of powders made up of micro-sized particles, Castellanos et al. proposed a balance equating the shear acting on the agglomerate to the van der Waals forces[145]:

$$\frac{\pi}{6}d_p^3\rho_p g\left(\frac{d_a}{d_p}\right)^{D_a+2}=\frac{A_{\mathrm{H}}d_p}{24z_0^2} \tag{26}$$

Rewriting Equation (26) gives:

$$d_a=\left(\frac{A_{\mathrm{h}}d_p^{D_a}}{4\pi\rho_p g z_0^2}\right)^{\frac{1}{D_a+2}} \tag{27}$$

Note that, since D_a has a positive value, this model predicts larger agglomerate sizes with an increase in primary particle size. It can also be seen that for this model single-step agglomeration is assumed to take place; agglomerates are directly made up of primary particles.

Mawatari et al. modelled agglomerate size of micro-sized powders in a vibro-fluidized bed.[105] Ignoring the effect of vibration, their model can be used to predict agglomerate sizes for micro-sized particles under unassisted conditions. The model is based on a balance between F_{vdW}, F_{D}, and F_g; when rewriting it to exclude the influence of vibration, their balance reduces to:

$$\frac{A_{\mathrm{H}}}{12z_0^2}\left(1+\frac{A_{\mathrm{H}}}{6\pi z_0^3\cdot H_r}\right)\cdot d_{\mathrm{asp}}=\frac{\pi}{6}d_a^3\left(\rho_a-\rho_f\right)g+3\pi\mu d_a u_{\mathrm{cha}}\varepsilon_{\mathrm{cha}}^{-3.8} \tag{28}$$

where H_r is the hardness of particle, taken to be $10^8\,\mathrm{N\,m^{-2}}$,[146] u_{cha} is the superficial gas velocity at which channels are broken, and $\varepsilon_{\mathrm{cha}}$ is the bed voidage at u_{cha}.

When looking at Equation (28) one can see it is derived by balancing F_{vdW} and $F_{\mathrm{W}}+F_{\mathrm{drag}}$, using Equation (6) and where F_{W} is corrected for buoyancy. One can also see that the primary particle size is not present in the equation, although it is known that it will influence the value of ρ_a.[145] Furthermore, when comparing Equations (28) with (26), it can also be seen that the calculation for F_{vdW} differs; Mawatari et al. used an equation for the van der Waals force from Krupp,[66,105] whereas Castellanos et al. used Equation (7). Also, Equation (28) is set up including both gravity and drag instead of just one of the two. The gravity needs to be overcome by the drag force in order to get the agglomerate to fluidize. When fluidization is taking place the forces are assumed to be equal[60,61]; one would therefore expect only one of the two to be present in the equation. Furthermore, the u_{cha} is a function of the cohesiveness of the powder, and therefore, indirectly, of d_p. Since no expression for u_{cha} was given, a sensitivity analysis could only be done with the assumption u_{cha} is constant with respect to d_p. For earlier discussed models, the density of the agglomerates was also a function of primary particle size, but Matawari et al. assumed the density to be constant, based on a study by Zhou and Li.[105,106]

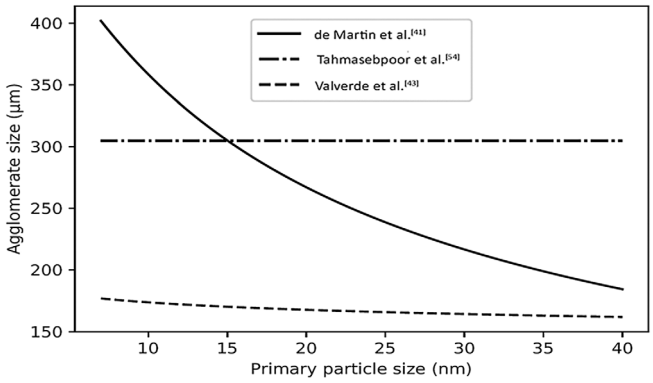

FIGURE 5 Predicted agglomerate size versus primary particle size; using parameters for hydrophobic SiO_2: $A_H = 1.5\cdot10^{-19}$ J, $z_0 = 4\cdot10^{-10}$ m, $d_{sa} = 3.5\cdot10^{-5}$m, $d_{\mathrm{asp}} = 2\cdot10^{-7}$m, $\rho_p = 2560\mathrm{kg/m^3}$, $\rho_b = 55\mathrm{kg/m^3}$, $g = 9.81\ \mathrm{m/s^2}$, $D_0 = 2.6$, $D_1 = 2.3$, $\widehat{N} = 1.2$

5.4 | Effect of primary particle sizes

Agglomerates are known to be formed by powders containing primary particles from a couple of nanometres up to tens of micrometres,[147] the latter sometimes falling into the Geldart type A classification.[30] This means that these agglomerates of larger primary particles fluidize easily, whereas the agglomerates made up of smaller primary particles usually do not. Therefore, the primary particle size must influence features of the formed agglomerates, causing the difference in fluidization behaviour. Differences in agglomerate size will be discussed in this section.

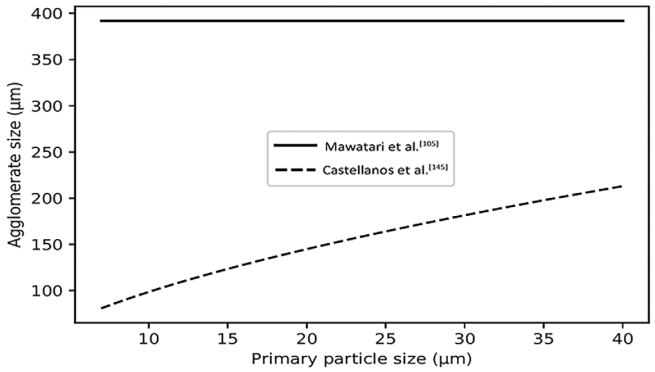

FIGURE 6 Predicted agglomerate size versus primary particle size; using parameters for hydrophobic SiO_2: $A_H = 1.5 \cdot 10^{-19}$ J, $z_0 = 4 \cdot 10^{-10}$ m, $D_a = 2.5$, $d_{asp} = 2 \cdot 10^{-7}$m, $\rho_p = 2560$ kg/m^3, $\rho_a = 55$kg/m^3, $\rho_f = 1.25$kg/m^3, $g = 9.81$ m/s^2, $u_{cha} = 5 \cdot 10^{-3}$m/s, $\varepsilon_{cha} = 0.75$, $H_r = 10^8$ N/m^2

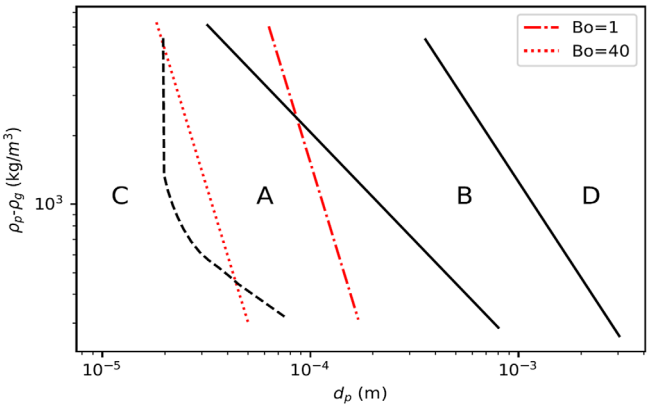

FIGURE 7 Geldart diagram with Bo = 1 plotted in red

In the previous section, we discussed some models to predict agglomerate size based on, among other things, primary particle size. Not all papers specified a range in which their models are thought to be accurate, but when plotting the predicted agglomerate sizes by the models developed for nano-sized primary particles in the range of 7–40 nm (the range in which the model by de Martín and van Ommen is accurate[41]) their results can be compared. From Figure 5 it can be seen that the models differ significantly in predicted agglomerate sizes. Furthermore, it can be seen that, whereas the model by Tahmasebpoor et al. is insensitive with respect to primary particle size, both the model by de Martín and van Ommen and by Valverde and Castellanos, predict a decrease in agglomerate size with increased primary particle size, though the slopes of the curves differ significantly.

The same was done for the models developed for agglomerates made up of micro-sized primary particles, shown in Figure 6. Here it can be seen that the model by Castellanos et al. predicts an increase in agglomerate size with increasing primary particle size, contrary to the models developed for nano-sized particles. None of the models can be correct throughout the entire size range in which agglomerates are formed. When extrapolating the models for nanoparticles they will end up predicting agglomerate sizes smaller than the primary particle size. Looking at the model by Castellanos et al. it predicts a decrease in agglomerate for smaller primary particles, whereas the value at 10 μm is already lower than the ones predicted by models for nanoparticles. The differences in the found trends are a result of the assumptions made in the models, specifically whether MSA is assumed to take place or not.

5.5 | Discussion

In order to develop a model, making assumptions is inevitable. However, one can argue that not all assumptions to be equally valid.

The most common, usually implicit, assumption is that agglomerates are perfectly spherical. From studies on this subject, it is known that the actual sphericity of agglomerates is about 0.7.[127] This assumption will change the drag force due to an underestimation of $A_\perp$. It will also change the effect of the van der Waals and capillary forces, although it is not easy to say what the effect is exactly.

Another thing to consider is that most models equate attractive forces to repulsive ones to calculate agglomerate size. Furthermore, models tend to use the van der Waals force as the only cohesive force and the drag force, which is equal to the weight force, as the only repulsive one. This means the models are, either explicitly or implicitly, assuming that an equilibrium is reached when the Bond number is equal to 1. The result of taking Bo = 1 and solving Equation (4) using Equations (3) and (9) is plotted in Figure 7. It can be seen that the solution to this equation falls well within the range of type A fluidization, whereas one would expect the powder to start fluidizing smoothly at the boundary between C to A already. Rhodes and colleagues proposed that the ratio between inter-agglomerate forces and the buoyant weight is larger than 40 for cohesive particles.[148] Note that, although Rhodes and colleagues did not use the term, this is the same as saying the Bond number is equal to 40. The solution to Bo = 40 is also plotted in Figure 7. It can be seen that this line is reasonably close to the boundary between type A and type C fluidization, meaning that solving Bo = 40 could give more representative results than solving Bo = 1. This could, however, change

when other inter-particle forces, namely those due to collisions, are taken into account.

One should also realize that the smallest freely moving entities present in the fluidized bed of nanopowders are aggregates, not the primary particles. Realizing that aggregate formation is dominated by production conditions,[149] not by particle properties, models based on aggregate features are likely to give more accurate results. Some of the found models did use the primary particle features to predict the aggregate size (often called sub-agglomerates), however, the properties of aggregates are a result of the production process and cannot be easily predicted based on primary particle properties alone.

Another shortcoming is the fact that, by the nature of the way most models are derived, they are only applicable in a certain range of particle sizes. Given that models are typically validated by experimental data in a narrow size range, the actual range in which the model is accurate is usually unknown. Limited applicability is obvious for models which assume MSA to take place, since they predict that an increase in d_p leads to a decrease in agglomerate size, meaning at some point the predicted agglomerate is predicted to be smaller than the primary particle, which is a non-physical result. The regime in which the MSA assumption is valid is not well identified. An ideal model, predicting agglomerate sizes based on material properties, particle size, and fluidization conditions, should include a transition between single and MSA based on a driving force. The underlying mechanism of MSA is, however, currently not fully understood. More research into this phenomenon is crucial for the further development of accurate models that are applicable over a larger size range.

Finally, in a balance, one equates attractive forces to repulsive ones, which implicitly assumes that an equilibrium between the forces exists in the bed. Given the fact that agglomerate sizes are known to change over time, as discussed in Section 4.2, it cannot be said that an equilibrium is present. This makes these balances inherently disputable for the prediction of agglomerate size.

6 | CONCLUSIONS AND OUTLOOK

As shown in this study, the fluidization of cohesive powders is complex and contains many sub-fields of research. Though much is known, there are still fundamental issues that require more insight for further development of the field.

Current classifications of powders, although useful, have limited reliability when it comes to predicting the fluidization behaviour of cohesive powders. As shown in this work, several different behaviours are found for type C powders alone. Furthermore, because cohesive powders form agglomerates, it is unclear whether the agglomerate properties or those of the primary particle should be used for predicting the fluidization behaviour. This is complicated even further when noting that the bed contains a distribution of agglomerate sizes, segregated over the bed height.

When it comes to predicting the sizes of formed agglomerates, multiple models have been proposed. They are, however, inconsistent with one another and at this time it cannot be said which are the more representative ones. The basic approach of balances to estimate agglomerate size is arguably flawed since this assumes an equilibrium to be present in the bed, whereas it is known that agglomerate sizes tend to change over time.

Overall it was found that micro- and nano-sized powders do indeed have some distinct characteristics and it is, to an extent, justified to treat them as such. The same inter-particle forces are dominant for both types of powders. The main difference is found in the way the powders form agglomerates: Nano-sized particles form multi-stage agglomerates, whereas micro-sized ones do not. This results in differences in the way these powders fluidize too.

To push the field of cohesive powder fluidization further, certain topics require more research. First of all, consensus should be reached on how to measure agglomerate sizes accurately. This will allow for data to be compared between studies as well as provide a strong basis for model validation. In order to come to a standard for size measurements, the dependency of agglomerate size on fluidization time should be studied rigorously too. Secondly, the phenomenon of MSA requires a fundamental understanding to develop models to predict agglomerate sizes for nanoparticles. This will also open the door for the development of generalized models which predict the agglomerate sizes of powders throughout larger size ranges including both nano- and microparticles.

NOMENCLATURE

Symbols

δ	deformation
γ	surface tension
γ_s	surface energy
μ	viscosity
ν	normal component of relative velocity
ρ_a	density of agglomerate
ρ_f	density of fluidizing gas
ρ_p	density of particle
ρ_{sa}	density of simple agglomerate
ε	bed voidage

φ	dimensionless inter-particle forces
A	surface area
a	contact radius
A_{H}	Hamaker constant
A_r	Archimedes number
B_o	Bond number
D	fractional dimension
d_a	diameter of agglomerate
d_p	diameter of particle
d_{asp}	diameter of asperity
d_{sa}	diameter of simple agglomerate
E^*	equivalent Young's modulus
F_{B}	buoyancy
F_{C}	collision force
F_{D}	drag force
F_{p}	pull-off force
$F_{\mu,n}$	viscous force
F_{IP}	inter-particle forces
F_{JKR}	van der Waals force, JKR model
F_{vdW}	van der Waals force
F_{W}	weight force
g	gravitational acceleration
H_0	minimum inter-particle distance
H_r	hardness
k_0, k_1	pre-factors for density ratio
l	azimuthal radius
N	number particles
$\widehat{N}$	fitting parameter
P	pressure
r	particle radius
R^*	equivalent radius
s	surface distance
u	superficial gas velocity
V	relative velocity
z_{eq}	equivalent distance

AUTHOR CONTRIBUTIONS

Rens Kamphorst: Writing – original draft. **Kaiqiao Wu:** Writing – original draft. **Samir Salameh:** Writing – original draft. **Gabrie M. H. Meesters:** Writing – review and editing. **J. Ruud van Ommen:** Writing – original draft; writing – review and editing.

ACKNOWLEDGEMENTS

With this paper, we would like to honour Prof. John R. Grace, who will always be remembered as a great leader in the field of chemical engineering, and specifically in fluidization technology. John combined being an inspiring and knowledgeable leader in the field with a very kind and modest personality. One of the authors, JRVO, cherishes the multiple times John made the effort to visit the group in Delft—for teaching in a course or serving in a PhD defence—and the several times John received him and his colleagues at UBC. John was not only a source of inspiration for us with his scientific work but also taught us by example about personal interaction and morality. We deeply miss him.

This work is part of the Advanced Research Center for Chemical Building Blocks, ARC CBBC, which is co-founded and co-financed by the Dutch Research Council (NWO) and the Netherlands Ministry of Economic Affairs and Climate Policy.

PEER REVIEW

The peer review history for this article is available at https://publons.com/publon/10.1002/cjce.24615.

DATA AVAILABILITY STATEMENT

Data sharing is not applicable to this article as no datasets were generated or analysed during the current study

REFERENCES

[1] A. Weir, P. Westerhoff, L. Fabricius, K. Hristovski, N. von Goetz, *Environ. Sci. Technol.* **2012**, *46*, 2242.
[2] S. Dekkers, H. Bouwmeester, P. M. Bos, R. J. Peters, A. G. Rietveld, A. G. Oomen, *Nanotoxicology* **2013**, *7*, 367.
[3] Y. Wang, L. Yuan, C. Yao, L. Ding, C. Li, J. Fang, K. Sui, Y. Liu, M. Wu, *Nanoscale* **2014**, *6*, 15333.
[4] S. Lehmann, E. U. Hartge, A. Jongsma, I. M. de Leeuw, F. Innings, S. Heinrich, *Powder Technol.* **2019**, *357*, 54.
[5] A. C. Burdusel, O. Gherasim, A. Grumezescu, L. Mogoantă, A. Ficai, E. Andronescu, *Nanomaterials* **2018**, *8*, 681.
[6] N. Zahin, R. Anwar, T. Twari, D. Kabir, A. Sajid, B. Mathew, S. Uddin, L. Aleya, M. Abdel-Daim, *Environ. Sci. Pollut. Res.* **2020**, *27*, 19151.
[7] H. Lu, J. Wang, M. Stoller, T. Wang, Y. Bao, H. Hao, *Adv. Mater. Sci. Eng.* **2016**, *2016*, 1.
[8] S. Tesh, T. Scott, *Adv. Mater.* **2014**, *26*, 6056.
[9] L. Chen, E. Hwang, J. Zhang, *Sensors* **2018**, *18*, 1440.
[10] V. Khanna, *Def. Sci. J.* **2018**, *2008*, 58.
[11] N. A. Lah, M. N. Zubir, M. A. Samykano, C. Mustansar Hussain, *Handbook of Nanomaterials for Industrial Applications, Micro and Nano Technologies*, Elsevier, Amsterdam, The Netherlands **2018**, p. 324.
[12] I. Matsui, *J. Chem. Eng. Jpn.* **2005**, *38*, 535.
[13] J. R. van Ommen, J. M. Valverde, R. Pfeffer, *J. Nanopart. Res.* **2012**, *14*, 737.
[14] F. Raganati, R. Chirone, P. Ammendola, *Chem. Eng. Res. Des.* **2018**, *133*, 347.
[15] J. R. Grace, *Introduction, History, and Applications*, John Wiley and Sons, Weinheim, Germany **2020**, p. 1.
[16] J. G. Yates, P. Lettieri, *Fluidized-Bed Reactors: Processes and Operating Conditions*, Springer International Publishing, Cham, Switzerland **2016**, p. 1.
[17] J. Wang, S. Wu, X.-K. Suo, H. Liao, in *Advanced Nanomaterials and Coatings by Thermal Spray, Micro and Nano Technologies* (Eds: G.-J. Yang, X. Suo), Elsevier, Amsterdam, The Netherlands **2019**, p. 13.
[18] S. Kang, M. Herzberg, D. F. Rodrigues, M. Elimelech, *Langmuir* **2008**, *24*, 6409.

[19] Y. Wang, L. Guohua, H. Yu, G. Gu, *Chem. Phys. Lett.* **2002**, *364*, 568.
[20] A. P. Rood, R. M. Scott, *Ann. Occup. Hyg.* **1989**, *33*, 583.
[21] M. Harper, E. G. Lee, S. S. Doorn, O. Hammond, *J. Occup. Environ. Hyg.* **2008**, *5*, 761.
[22] European Union (EU), *Off. J. Eur. Communities: Legis.* **2011**, *54*, 38.
[23] O. Amjadi, M. Tahmasebpoor, H. Aghdasinia, *Chem. Eng. Technol.* **2019**, *42*, 287.
[24] H. Liu, Y. Li, Q. Guo, *Ind. Eng. Chem. Res.* **2006**, *45*, 1805.
[25] L. Song, T. Zhou, J. Yang, *Adv. Powder Technol.* **2009**, *20*, 366.
[26] H. Mo, B. Xu, C. Luo, T. Zhou, J. Kong, *Chin. J. Chem. Eng.* **2018**, *26*, 2531.
[27] J. R. Grace, G. Sun, *Can. J. Chem. Eng.* **1991**, *69*, 1126.
[28] G. Khoe, T. Ip, J. Grace, *Powder Technol.* **1991**, *66*, 127.
[29] R. Beetstra, J. Nijenhuis, N. Ellis, J. R. van Ommen, *AIChE J.* **2013**, *2009*, 55.
[30] D. Geldart, *Powder Technol.* **1973**, *7*, 285.
[31] S. Morooka, K. Kusakabe, A. Kobata, Y. Kato, *J. Chem. Eng. Jpn.* **1988**, *21*, 41.
[32] A. Pacek, A. Nienow, *Powder Technol.* **1990**, *60*, 145.
[33] W. Yao, G. Guangsheng, W. Fei, W. Jun, *Powder Technol.* **2002**, *124*, 152.
[34] J. Valverde, A. Castellanos, *AIP Conf. Proc.* **2009**, *1145*, 977.
[35] C. Zhu, Q. Yu, R. Dave, R. Pfeffer, *AIChE J.* **2005**, *51*, 426.
[36] J. R. Grace, *Can. J. Chem. Eng.* **1986**, *64*, 353.
[37] W.-C. Yang, *Powder Technol.* **2007**, *171*, 69.
[38] W. R. Goossens, *Powder Technol.* **1998**, *98*, 48.
[39] N. Mostoufi, *Chem. Eng. Sci.* **2020**, *229*, 116029.
[40] S. Matsuda, H. Hatano, T. Muramoto, A. Tsutsumi, *AIChE J.* **2004**, *50*, 2763.
[41] L. de Martín, J. R. van Ommen, *J. Nanopart. Res.* **2013**, *15*, 2055.
[42] H. Liu, L. Zhang, T. Chen, S. Wang, Z. Han, S. Wu, *Chem. Eng. J.* **2015**, *262*, 579.
[43] J. M. Valverde, M. A. S. Quintanilla, A. Castellanos, D. Lepek, J. Quevedo, R. N. Dave, R. Pfeffer, *AIChE J.* **2008**, *54*, 86.
[44] S. V. Sokolov, E. Kätelhön, R. G. Compton, *J. Phys. Chem. C* **2015**, *119*, 25093.
[45] A. Fabre, A. Clemente, F. Balas, M. P. Lobera, J. Santamaría, M. T. Kreutzer, J. R. van Ommen, *Environ. Sci.: Nano* **2017**, *4*, 1591.
[46] X. Zhang, Y. Zhou, J. Zhu, *Powder Technol.* **2021**, *377*, 684.
[47] A. Kamranian Marnani, A. Bück, S. Antonyuk, B. van Wachem, D. Thévenin, J. Tomas, *Processes* **2019**, *7*, 35.
[48] T. Zhou, H. Li, *Powder Technol.* **1999**, *102*, 215.
[49] Z. Wang, M. Kwauk, H. Li, *Chem. Eng. Sci.* **1998**, *53*, 377.
[50] S. Kaliyaperumal, S. Barghi, L. Briens, S. Rohani, J. Zhu, *Particuology* **2011**, *9*, 279.
[51] C. Mogre, A. U. Thakurdesai, J. R. van Ommen, S. Salameh, *Powder Technol.* **2017**, *316*, 441.
[52] E. Hotze, T. Phenrat, G. Lowry, *J. Environ. Qual.* **1909**, *2010*, 39.
[53] K. Rietema, in *The Dynamics of Fine Powders*, Springer, Dordrecht, The Netherlands **1991**.
[54] M. Tahmasebpoor, R. G. S. Abadi, Y. R. Noupoor, P. Badamchizadeh, *Ind. Eng. Chem. Res.* **2016**, *55*, 12939.
[55] J. Seville, C. Willett, P. Knight, *Powder Technol.* **2000**, *113*, 261.
[56] M. Tahmasebpoor, L. de Martín, M. Talebi, N. Mostoufi, J. R. van Ommen, *Phys. Chem. Chem. Phys.* **2013**, *15*, 5788.
[57] S. Leroch, M. Wendland, *Langmuir* **2013**, *29*, 12410.
[58] S. C. Endres, L. C. Ciacchi, L. Mädler, *J. Aerosol Sci.* **2021**, *153*, 105719.
[59] M. Capece, R. Ho, J. Strong, P. Gao, *Powder Technol.* **2015**, *286*, 561.
[60] J. Chaouki, C. Chavarie, D. Klvana, G. Pajonk, *Powder Technol.* **1985**, *43*, 117.
[61] J. Shabanian, R. Jafari, J. Chaouki, *Int. Rev. Chem. Eng.* **2012**, *4*, 16.
[62] P. Foscolo, L. Gibilaro, *Chem. Eng. Sci.* **1984**, *39*, 1667.
[63] M. R. Tamadondar, R. Zarghami, K. Boutou, M. Tahmasebpoor, N. Mostoufi, *Can. J. Chem. Eng.* **2016**, *94*, 476.
[64] O. Walton, *Kona Powder Part. J.* **2008**, *26*, 129.
[65] J. Israelachvili, *Intermolecular and Surface Forces*, Academic Press, Burlington, VT **2011**.
[66] H. Krupp, *Adv. Colloid Interface Sci.* **1967**, *1*, 111.
[67] K. Jiang, P. Pinchuk, *Nanotechnology* **2016**, *27*, 345710.
[68] J. R. van Ommen, A. Goulas, *Mater. Today Chem.* **2019**, *14*, 100183.
[69] R. Chirone, M. Poletto, D. Barletta, P. Lettieri, *Powder Technol.* **2020**, *362*, 307.
[70] P. Lettieri, D. Macrì, *Kona Powder Part. J.* **2016**, *33*, 86.
[71] L. Zhou, F. Zhang, H. Kage, Y. Mawatari, *Korean J. Chem. Eng.* **2013**, *30*, 501.
[72] S. Matsuda, H. Hatano, A. Tsutsumi, *Chem. Eng. J.* **2001**, *82*, 183.
[73] M. Espín, J. M. Valverde, M. Quintanilla, A. Castellanos, *Phys. Rev. E* **2009**, *79*, 011304.
[74] Y. I. Rabinovich, J. J. Adler, A. Ata, R. K. Singh, B. M. Moudgil, *J. Colloid Interface Sci.* **2000**, *232*, 10.
[75] K. Gong, L. Chen, H. Xia, H. Dai, X. Li, L. Sun, W. Kong, K. Liu, *Int. J. Biol. Macromol.* **2019**, *130*, 915.
[76] P. Liu, C. Q. LaMarche, K. M. Kellogg, C. M. Hrenya, *Physical Review Fluids* **2017**, *2*, 054302.
[77] H. C. H. Rumpf, *Chem. Ing. Tech.* **1970**, *42*, 538.
[78] C. Q. LaMarche, S. Leadley, P. Liu, K. M. Kellogg, C. M. Hrenya, *Chem. Eng. Sci.* **2017**, *158*, 140.
[79] J. E. Galvin, S. Benyahia, *AIChE J.* **2014**, *60*, 473.
[80] K. L. Johnson, K. Kendall, A. D. Roberts, D. Tabor, *Proc. R. Soc. A* **1971**, *324*, 301.
[81] J. Yang, C.-Y. Wu, M. Adams, *Acta Pharm. Sin. B* **2014**, *4*, 52.
[82] J. Yang, C.-Y. Wu, M. Adams, *Int. J. Pharm.* **2015**, *487*, 32.
[83] M. W. Weber, D. K. Hoffman, C. M. Hrenya, *Granular Matter* **2004**, *6*, 239.
[84] P. Liu, C. Q. LaMarche, K. M. Kellogg, C. M. Hrenya, *AIChE J.* **2018**, *64*, 2329.
[85] S. Salameh, M. A. van der Veen, M. Kappl, J. R. van Ommen, *Langmuir* **2017**, *33*, 2477.
[86] H.-J. Butt, M. Kappl, *Adv. Colloid Interface Sci.* **2009**, *146*, 48.
[87] Y. Li, J. Hu, K. Bai, *J. Adhes. Sci. Technol.* **2015**, *30*, 1.
[88] O. Pakarinen, A. Foster, M. Paajanen, T. Kalinainen, J. Katainen, I. Makkonen, J. Lahtinen, R. Nieminen, *Modell. Simul. Mater. Sci. Eng.* **2005**, *13*, 1175.
[89] M. Dörmann, H.-J. Schmid, *Powder Technol.* **2017**, *312*, 175.
[90] S. Salameh, J. Schneider, J. Laube, A. Alessandrini, P. Facci, J. W. Seo, L. Ciacchi, L. Mädler, *Langmuir* **2012**, *28*, 11457.
[91] S. Plimpton, *J. Comput. Phys.* **1995**, *117*, 1.

[92] V. S. Sutkar, N. G. Deen, J. T. Padding, J. Kuipers, V. Salikov, B. Crüger, S. Antonyuk, S. Heinrich, *AIChE J.* **2015**, *61*, 769.
[93] B. Crüger, V. Salikov, S. Heinrich, S. Antonyuk, V. S. Sutkar, N. G. Deen, J. Kuipers, *Particuology* **2016**, *25*, 1.
[94] P. Darabi, K. Pougatch, M. Salcudean, D. Grecov, *Powder Technol.* **2011**, *214*, 365.
[95] M. Farshchi-Tabrizi, M. Kappl, Y. Cheng, J. Gutmann, H.-J. Butt, *Langmuir* **2006**, *22*, 2171.
[96] H.-J. Butt, M. Kappl, *Surface and Interfacial Forces*, 2nd ed., Wiley-VCH, Weinheim, Germany **2010**.
[97] N. V. Zarate, A. J. Harrison, J. D. Litster, S. P. Beaudoin, *J. Colloid Interface Sci.* **2013**, *411*, 265.
[98] H.-J. Butt, W. J. P. Barnes, A. del Campo, M. Kappl, F. Schönfeld, *Soft Matter* **2010**, *6*, 5930.
[99] T. Gröger, U. Tüzün, D. M. Heyes, *Powder Technol.* **2003**, *133*, 203.
[100] R. Pfeffer, J. A. Queyedo, *U.S. Patent 7905433*, **2011**.
[101] J. Peart, *Kona Powder Part. J.* **2001**, *19*, 34.
[102] A. Bailey, *J. Electrost.* **1993**, *30*, 167.
[103] A. Bailey, *Powder Technol.* **1984**, *37*, 71.
[104] J. Valverde, M. Quintanilla, M. Espín, A. Castellanos, *Phys. Rev. E: Stat. Phys., Plasmas, Fluids, Relat. Interdiscip. Top.* **2008**, *77*, 031301.
[105] Y. Mawatari, T. Ikegami, Y. Tatemoto, K. Noda, *J. Chem. Eng. Jpn.* **2003**, *36*, 277.
[106] T. Zhou, H. Li, *Powder Technol.* **1999**, *101*, 57.
[107] Y. Horio, M. Iwadate, in *Proc. of the 5th World Congress of Chemical Engineering: 2nd Int. Particle Technology Forum*, Vol. V, American Institute of Chemical Engineers, San Diego, CA **1996**, p. 571.
[108] X. Jiang, Q. Zeng, C. Chen, A. Yu, *J. Mater. Chem.* **2011**, *21*, 16797.
[109] R. A. Bowling, *A Theoretical Review of Particle Adhesion*, Springer, Boston, MA **1988**, p. 129.
[110] J. P. Seville, U. Tüzün, R. Clift, *Processing of Particulate Solids*, Champan & Hall, London, UK **1997**, p. 120.
[111] B. van Wachem, S. Sasic, *AIChE J.* **2008**, *54*, 9.
[112] L. Niu, Z. Chu, M. Cai, M. Liu, *Ind. Eng. Chem. Res.* **2019**, *58*, 8472.
[113] A. A. Motlagh, J. R. Grace, M. Salcudean, C. Hrenya, *Chem. Eng. Sci.* **2014**, *120*, 22.
[114] A. Teleki, R. Wengeler, L. Wengeler, H. Nirschl, S. Pratsinis, *Powder Technol.* **2008**, *181*, 292.
[115] C. Nam, R. Pfeffer, R. Dave, S. Sundaresan, *AIChE J.* **2004**, *50*, 1776.
[116] L. F. Hakim, S. M. George, A. W. Weimer, *Nanotechnology* **2005**, *16*, S375.
[117] G. P. Cherepanov, *Physics of Sintering*, Springer, Dordrecht, The Netherlands **1997**, p. 84.
[118] A. Gutsch, M. Krämer, G. Michael, H. Mühlenweg, M. Pridöhl, G. Zimmermann, *Kona Powder Part. J.* **2002**, *20*, 24.
[119] F. E. Kruis, K. A. Kusters, S. E. Pratsinis, B. Scarlett, *Aerosol Sci. Technol.* **1993**, *19*, 514.
[120] D. Walter, *Primary Particles—Agglomerates—Aggregates*, John Wiley and Sons, Weinheim, Germany **2013**, p. 9.
[121] G. D. Ulrich, N. S. Subramanian, *Combust. Sci. Technol.* **1977**, *17*, 119.
[122] M.-G. Li, C.-J. Sun, S.-H. Gau, C.-J. Chuang, *J. Hazard. Mater.* **2009**, *174*, 586.
[123] L. Wang, S. Liu, Y. Hou, S. Lang, C. Wang, D. Zhang, *J. Food Process. Preserv.* **2020**, *44*, e14569.
[124] R. Sarrate, J. R. Ticó, M. Miñarro, C. Carrillo, A. Fàbregas, E. García-Montoya, P. Pérez-Lozano, J. M. Suñé-Negre, *Powder Technol.* **2015**, *270*, 244.
[125] J. Toro-Sierra, J. Schumann, U. Kulozik, *Dairy Sci. Technol.* **2013**, *93*, 487.
[126] S. S. Ali, A. Arsad, M. Asif, *Chem. Eng. Process.* **2021**, *159*, 108243.
[127] X. Wang, V. Palero, J. Soria, M. Rhodes, *Chem. Eng. Sci.* **2006**, *61*, 5476.
[128] J. Quevedo, R. Pfeffer, *Ind. Eng. Chem. Res.* **2010**, *49*, 5263.
[129] L. de Martín, J. Sánchez-Prieto, F. Hernández-Jiménez, J. R. van Ommen, *J. Nanopart. Res.* **2014**, *16*, 1.
[130] R. Hong, J. Ding, H. Li, *China Particuol.* **2005**, *3*, 181.
[131] J. R. van Ommen, D. King, A. Weimer, R. Pfeffer, B. van Wachem, presented at The 13th Int. Conf. on Fluidization, Hotel Hyundai, Gyeong-ju, Korea, May **2010**.
[132] H. Nasri Lari, J. Chaouki, J. R. Tavares, *Powder Technol.* **2017**, *316*, 455.
[133] J. Quevedo, A. Omosebi, R. Pfeffer, *AIChE J.* **2009**, *56*, 1456.
[134] Q. Guo, H. Liu, W. Shen, X. Yan, R. Jia, *Chem. Eng. J.* **2006**, *119*, 1.
[135] E. AL-Ghurabi, M. Shahabuddin, N. S. Kumar, M. Asif, *Nanomaterials* **2020**, *10*, 388.
[136] S. Ali, E. AL-Ghurabi, A. Ajbar, Y. Mohammed, M. Boumaza, M. Asif, *J. Nanomater.* **2016**, *2016*, 1.
[137] S. S. Ali, M. Asif, *Powder Technol.* **2012**, *225*, 86.
[138] F. Zhang, D. La Zara, F. Sun, M. J. Quayle, G. Petersson, S. Folestad, J. R. van Ommen, *Can. J. Chem. Eng.* **2021**, *99*, 1696.
[139] L. D. Martín, W. G. Bouwman, J. R. van Ommen, *AIP Conf. Proc.* **2013**, *1542*, 82.
[140] A. Castellanos, J. M. Valverde, M. A. S. Quintanilla, *Phys. Rev. E* **2001**, *64*, 041304.
[141] J. Quevedo, R. Pfeffer, Y. Shen, R. Dave, H. Nakamura, S. Watano, *AIChE J.* **2006**, *52*, 52.
[142] J. M. Valverde, A. Castellanos, *Powder Technol.* **2008**, *181*, 347.
[143] M. A. S. Quintanilla, J. M. Valverde, M. J. Espin, A. Castellanos, *Ind. Eng. Chem. Res.* **2012**, *51*, 531.
[144] J. M. Valverde, A. Castellanos, *Chem. Eng. Sci.* **2007**, *62*, 6947.
[145] A. Castellanos, J. M. Valverde, M. Quintanilla, *Phys. Rev. Lett.* **2005**, *94*, 075501.
[146] O. Molerus, *Powder Technol.* **1982**, *33*, 81.
[147] M. Horio, H. Kuroki, *Chem. Eng. Sci.* **1994**, *49*, 2413.
[148] X. Wang, F. Rahman, M. Rhodes, *Chem. Eng. Sci.* **2007**, *62*, 3455.
[149] H. Barthel, L. Rösch, J. Weis, *Fumed Silica–Production, Properties, and Applications, Chapter*, Vol. 91, John Wiley and Sons, Weinheim, Germany **1995**, p. 761.

How to cite this article: R. Kamphorst, K. Wu, S. Salameh, G. M. H. Meesters, J. R. van Ommen, *Can. J. Chem. Eng.* **2022**, 1. https://doi.org/10.1002/cjce.24615